

- Neubig, R. R., Krodell, E. K., Boyd, N. D., & Cohen, J. B. (1979) *Proc. Natl. Acad. Sci. U.S.A.* 76, 690-694.
- O'Farrell, P. H. (1975) *J. Biol. Chem.* 250, 4007-4021.
- Parker, P., Coussens, L., Totty, U., Rhee, L., Young, S., Chen, E., Stubel, S., Waterfield, M., & Ullrich, A. (1986) *Science (Washington, D.C.)* 233, 853-859.
- Pedersen, S. E., Dreyer, E. B., & Cohen, J. B. (1986) *J. Biol. Chem.* 261, 13735-13743.
- Peng, H. B., & Froehner, S. C. (1985) *J. Cell Biol.* 100, 1698-1705.
- Perryman, M. B., Knell, J. D., Ifegwu, J., & Roberts, R. (1985) *J. Biol. Chem.* 260, 9399-9404.
- Porter, S., & Froehner, S. C. (1983) *J. Biol. Chem.* 258, 10034-10040.
- Porter, S., & Froehner, S. C. (1985) *Biochemistry* 24, 425-432.
- Rousselet, A., Cartaud, J., & Devaux, P. F. (1981) *Biochim. Biophys. Acta* 648, 169-185.
- Saitoh, T., Wennogle, L. P., & Changeux, J.-P. (1979) *FEBS Lett.* 108, 489-494.
- Schaffner, W., & Weissman, C. (1973) *Anal. Biochem.* 56, 502-504.
- Sealock, R., Wray, B. E., & Froehner, S. C. (1984) *J. Cell Biol.* 98, 2239-2244.
- Smyth, D. G., Stein, W. A., & Moore, S. (1963) *J. Biol. Chem.* 238, 227-234.
- Sobel, A., Weber, M., & Changeux, J.-P. (1977) *Eur. J. Biochem.* 80, 215-224.
- Sobel, A., Heidman, T., Hofler, J., & Changeux, J.-P. (1978) *Proc. Natl. Acad. Sci. U.S.A.* 75, 510-514.
- Steffens, G., Gunzler, W., Otting, F., Franks, E., & Flohe, L. (1982) *Hoppe-Seyler's Z. Physiol. Chem.* 363, 1043-1058.
- St. John, P. A., Froehner, S. C., Goodenough, D. A., & Cohen, J. B. (1982) *J. Cell Biol.* 92, 333-342.
- Takio, K., Blumenthal, D., Walsh, K., Titani, K., Krebs, E. (1986) *Biochemistry* 25, 8049-8057.
- Towler, D., Adams, S., Eubanks, S., Towery, D., Jackson-Machelski, E., Glaser, L., & Gordon, J. (1987) *Proc. Natl. Acad. Sci. U.S.A.* 84, 2708-2712.
- Walker, J. H., Boustead, C. M., & Witzemann, V. (1984) *EMBO J.* 3, 2287-2290.
- Wennogle, L. P., & Changeux, J.-P. (1980) *Eur. J. Biochem.* 106, 381-393.

Electron Transfer from Cytochrome b_5 to Iron and Copper Complexes[†]

Lorne S. Reid,^{†,§} Harry B. Gray,[‡] Claudio Dalvit,^{||} Peter E. Wright,^{||} and Paul Saltman^{*,‡}

Arthur Amos Noyes Laboratory, California Institute of Technology, Pasadena, California 91125, Department of Molecular Biology, Research Institute of Scripps Clinic, La Jolla, California 92037, and Department of Biology, University of California, San Diego, La Jolla, California 92092

Received March 9, 1987; Revised Manuscript Received June 22, 1987

ABSTRACT: The rates of electron transfer from the tryptic fragment of bovine liver cytochrome b_5 to $\text{Fe}^{\text{III}}\text{NTA}$, $\text{Fe}^{\text{III}}\text{ATP}$, $\text{Cu}^{\text{II}}\text{NTA}$, $\text{Cu}^{\text{II}}\text{ATP}$, and $\text{Cu}^{\text{II}}\text{His}$ have been measured by anaerobic stopped-flow techniques. The rates of reduction of the $\text{Fe}(\text{III})$ complexes are independent of ionic strength, enhanced at low pH, and slightly inhibited by $\text{Zn}^{\text{II}}\text{NTA}$. Saturation kinetics are observed with $\text{Cu}^{\text{II}}\text{NTA}$ ($k_{\text{et}} = 0.05 \text{ s}^{-1}$, $K = 8.6 \text{ M}^{-1}$), $\text{Cu}^{\text{II}}\text{His}$ ($k_{\text{et}} = 0.2 \text{ s}^{-1}$, $K = 2.6 \times 10^3 \text{ M}^{-1}$), and $\text{Cu}^{\text{II}}\text{ATP}$ ($k_{\text{et}} = 0.6 \text{ s}^{-1}$, $K = 4.5 \times 10^3 \text{ M}^{-1}$), thereby indicating that binding of $\text{Cu}(\text{II})$ to the protein occurs prior to electron transfer. ^1H NMR resonances of the three surface histidines and some neighboring residues have been assigned by two-dimensional NMR techniques. NMR titration experiments show unequivocally that $\text{Cu}^{\text{II}}\text{NTA}$ binds preferentially at a site near His-26 and Tyr-27.

It has been demonstrated that cytochrome b_5 is reduced by $\text{Fe}^{\text{II}}\text{EDTA}^1$ through direct transfer of an electron at the exposed heme edge (Reid & Mauk, 1982). A similar mechanism is employed in the reduction of $\text{Fe}^{\text{III}}\text{NTA}$ by myoglobin (Hegetschweiler et al., 1987). A very different pathway, however, is utilized in the oxidation of hemoglobin β chains

by $\text{Cu}^{\text{II}}\text{NTA}$ (Rifkind, 1981). Subsequent to $\text{Cu}(\text{II})$ binding to Cys-93, an electron apparently is transferred a long distance from $\text{Fe}(\text{II})$ to $\text{Cu}(\text{II})$. The plausibility of a long-range mechanism for the $\text{Cu}^{\text{II}}\text{NTA}$ oxidation of hemoglobin has been strengthened by the observation of 10-25-Å electron transfers in fixed-distance experiments on several heme proteins (Mayo et al., 1986).

We have employed anaerobic stopped-flow techniques to measure the rates of electron transfer from the tryptic fragment of bovine liver cytochrome b_5 to $\text{Fe}^{\text{III}}\text{NTA}$, $\text{Fe}^{\text{III}}\text{ATP}$, $\text{Cu}^{\text{II}}\text{NTA}$, $\text{Cu}^{\text{II}}\text{ATP}$, and $\text{Cu}^{\text{II}}\text{His}$. The evidence reported here suggests that a long-range pathway is utilized in the b_5 to $\text{Cu}(\text{II})$ electron transfers.

[†] This work was supported in part by National Institutes of Health Grants AM34909 and AM12386. Research at the California Institute of Technology (Contribution No. 7612) was supported by NIH Grant DK-19038. A preliminary account of this work was presented at the Annual Meeting of the Federation of American Societies for Experimental Biology, Washington, DC, June 1986.

[‡] California Institute of Technology.

[§] Present address: Laboratory of Molecular Biology, Department of Crystallography, Birkbeck College, London, WC1E 7HX England.

^{||} Research Institute of Scripps Clinic.

^{*} University of California, San Diego.

¹ Abbreviations: EDTA, ethylenediaminetetraacetic acid; NTA, nitrilotriacetic acid; Hepes, 4-(2-hydroxymethyl)-1-piperazineethanesulfonic acid.

MATERIALS AND METHODS

Reagents. The tryptic fragment of cytochrome b_5 was prepared as described previously (Reid & Mauk, 1982), purified to $R_{412.5/280} \geq 5.85$, and stored in liquid nitrogen. NTA, ATP, and histidine were purchased from Sigma; all other chemicals were of reagent quality. Distilled water was further purified to a conductivity of $>17 \text{ M}\Omega \text{ cm}^{-1}$ over a Barnsted NANO pure water purifier immediately prior to use. Hepes buffer was prepared at 20 mM; the ionic strength was adjusted by the addition of NaCl.

Stock solutions of chelators [NTA, ATP, His] and metal salts [FeCl_3 , CuSO_4 , ZnSO_4 , NiCl_2] were prepared in distilled water. Stock solutions (1 mM) of the metal chelates were prepared by adding the metal salt to the chelate with continuous stirring. The pH of the solution was adjusted to 5.5 with a stock solution of 1 M NaHCO_3 and then to the working pH value with 1 N NaOH before bringing to volume with distilled water. The Fe^{III} NTA solutions were protected from exposure to light.

Measurements. All solutions were thoroughly degassed by bubbling with argon, previously deoxygenated by bubbling through two methyl viologen and one photoreduced proflavin scrubbing tower. Solutions were then transferred anaerobically to a modified Durrum-Gibson stopped-flow spectrophotometer (Reid & Mauk, 1982). All protein solutions contained 3 mM cytochrome b_5 , 10 mM chelate, 1 μM methyl viologen, and 1 μM proflavin. The cytochrome b_5 solutions were photoreduced in situ by irradiation with a 100-W incandescent lamp situated 15 cm from the reaction tube (Bonfils et al., 1981). The reduction was complete within the 25-min period used to equilibrate the sample to temperature; a circulating water bath was used to stabilize the temperature to ± 0.2 deg. When temperatures other than 25 °C were used, the time for equilibration was increased to 45 min. The chelate solutions were used at pseudo-first-order concentrations of at least 10:1 (chelate:protein). Generally, 10 shots could be achieved from a single barrel in the stopped-flow spectrophotometer (the resultant decay curves were signal-averaged). Absorbance decay curves at 412.5 nm (increase in oxidized cytochrome b_5) and at 423 nm (loss of reduced cytochrome b_5) were compared and found to give the same rate constants. Data were collected by an On-Line-Instrument-Systems (OLIS) 3820 microcomputer system. Nonlinear analysis of first-order rate constants was performed by the OLIS stopped-flow data collection/analysis program (SFLOW, Rev 2.0) on the collected decay curves.

Quantitative spectrophotometric measurements were made on a Cary 219 spectrophotometer. Concentrations of Fe and Cu in the chelate solutions were checked by quantitative flame atomic absorption methods.

Samples of protein were prepared for ^1H NMR analysis by exchanging the solution repeatedly with deuterated potassium phosphate buffer (p ^2H 7.0) in a YM 5 Centricron unit. Solutions of Cu^{II} NTA in $^2\text{H}_2\text{O}$ were prepared as described above. ^1H NMR spectra were obtained on a Bruker AM500 spectrometer equipped with digital phase shifting hardware. Spectra were recorded for oxidized cytochrome b_5 in $^2\text{H}_2\text{O}$ at p ^2H 6.9 (24 °C). Stated p ^2H values refer to uncorrected meter readings. Dioxane was used as an internal standard, but all chemical shifts are referred to (trimethylsilyl)propanesulfonic acid. A phase-sensitive double-quantum spectrum was recorded by using the standard pulse sequence (Braunschweiler et al., 1983) with a $\pi/2$ detection pulse and double-quantum excitation period $\tau = 40$ ms. A total of 512 t_1 values were recorded with 64 scans at each value of t_1 . A phase-sensitive

Table I: Rate Constants for Reduction of Fe^{III} Complexes by Cytochrome b_5 at 25 °C (pH 7.0)

complex	μ (M)	$k_{12} (\times 10^{-3} \text{ M}^{-1} \text{ s}^{-1})$
Fe^{III} NTA	0.05	1.27 ± 0.1
	0.1	1.51 ± 0.05
	0.2	1.44 ± 0.1
	0.3	1.43 ± 0.05
Fe^{III} ATP	0.1	0.90 ± 0.03

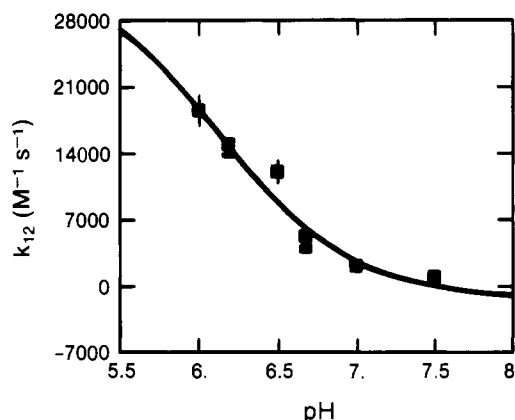


FIGURE 1: Dependence of the second-order rate constant on pH for the reduction of Fe^{III} NTA by cytochrome b_5 at 25 °C ($\mu = 0.1 \text{ M}$ Hepes). The fit is for a $\text{p}K_a$ of 6.2.

relayed coherence transfer spectrum was recorded with the pulse sequence of Eich et al. (1982). Standard phase cycling was used to eliminate undesired axial peaks and nuclear Overhauser effects (Wagner, 1983) except that the phase of the first two $\pi/2$ pulses was varied while that of the last $\pi/2$ pulse was kept constant. A mixing time $\tau = 25$ ms was employed. A phase-sensitive NOESY spectrum (Kumar et al., 1980) was recorded with a mixing time $\tau = 200$ ms. A total of 996 t_1 values was acquired with 64 scans at each t_1 increment. For all two-dimensional NMR experiments, quadrature detection in ω_1 was achieved with time proportional phase incrementation.

Evans and Sutherland PS300 interactive graphics (Department of Crystallography, Birkbeck College, University of London) were used to study the docking of copper complexes onto cytochrome b_5 . The solvent-accessible protein surface was calculated with a 1.4-Å probe. Interactive docking of the complexes onto the protein was accomplished with the program HYDRA.

Atomic coordinates were obtained for cytochrome b_5 from the Brookhaven protein database (2B5C) and for the copper complexes from the Cambridge database: Cu^{II} NTA·Na· H_2O (SCNTAC10) and Cu^{II} His· Cl_2 (BCLDUB).

RESULTS AND DISCUSSION

Electron Transfer to Fe^{III} . The rate of electron transfer from cytochrome b_5 to Fe^{III} NTA is not affected by changes in ionic strength. Five different chelate:protein concentration ratios (10:1 to 400:1 mol/mol) were used at each ionic strength. Plots of k_{obsd} vs. $[\text{Fe}^{\text{III}}$ NTA] were linear with zero intercepts. Second-order rate constants for the reactions of Fe^{III} NTA and of Fe^{III} ATP are given in Table I. The rate of reduction of Fe^{III} NTA was slightly inhibited in the presence of Zn^{II} NTA, whereas Ni^{II} NTA had no effect.

The pH dependence of the second-order rate constant for reduction of Fe^{III} NTA is shown in Figure 1. The data have been fit to eq 1 in a manner similar to that previously described

$$k_{12} = \frac{k_a[\text{H}^+] + k_b[\text{K}_a]}{[\text{H}^+] + \text{K}_a} \quad (1)$$

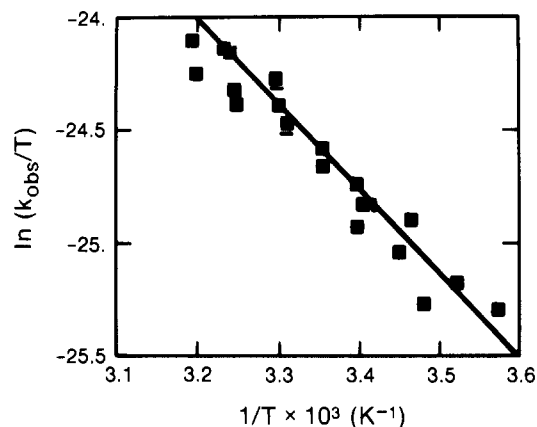


FIGURE 2: Eyring plot for the reduction of $\text{Fe}^{\text{III}}\text{NTA}$ by cytochrome b_5 (pH 7.5, $\mu = 0.1$ M Hepes).

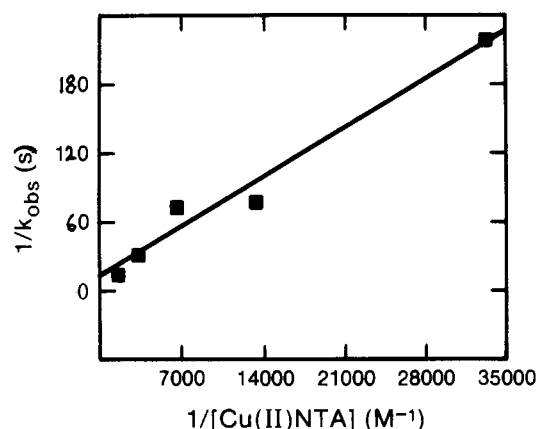


FIGURE 3: Double-reciprocal plot for the reduction of $\text{Cu}^{\text{II}}\text{NTA}$ by cytochrome b_5 at 25 °C (pH 7.0, $\mu = 0.1$ M).

(Reid & Mauk, 1982). The pK_a of 6.2 could be associated with a water coordinated to $\text{Fe}^{\text{III}}\text{NTA}$ (Hegetschweiler et al., 1987). Since uncharged $\text{Fe}^{\text{III}}\text{NTA}$ (midpoint potential of 330 mV) is a stronger oxidant than is $\text{Fe}^{\text{III}}\text{NTA}(\text{OH})^-$ ($E_m^\circ \sim 0$ mV), the observed increase in the electron-transfer rate at low pH accords with expectation. The pH was not taken below 6.0 due to the instability of the protein under acidic conditions.

The temperature dependence of the rate constant for the reduction of $\text{Fe}^{\text{III}}\text{NTA}$ by cytochrome b_5 is shown in Figure 2. The activation parameters ($\Delta H^\ddagger = 6.7 \pm 0.2$ kcal/mol, $\Delta S^\ddagger = -21.7 \pm 0.8$ eu) are similar to those obtained for the reduction of cytochrome b_5 by $\text{Fe}^{\text{II}}\text{EDTA}$ ($\Delta H^\ddagger = 5.4 \pm 0.2$ kcal/mol, $\Delta S^\ddagger = -29.2 \pm 0.2$ eu) (Reid & Mauk, 1982).

Electron Transfer to $\text{Cu}(\text{II})$. All of the $\text{Cu}(\text{II})$ oxidations of cytochrome b_5 exhibited saturation kinetics. A representative double-reciprocal plot is shown in Figure 3. It is probable that $\text{Cu}(\text{II})$ binding to the protein occurs prior to electron transfer. The rate constants and binding constants for the oxidation of cytochrome b_5 by $\text{Cu}^{\text{II}}\text{NTA}$, $\text{Cu}^{\text{II}}\text{ATP}$, and $\text{Cu}^{\text{II}}\text{His}$ are set out in Table II. The $\text{Cu}^{\text{II}}\text{NTA}$ reduction is slightly enhanced at higher ionic strengths (Table II). $\text{Zn}^{\text{II}}\text{NTA}$ inhibits the reduction.

The temperature dependence of the rate constant for the reaction of cytochrome b_5 with $\text{Cu}^{\text{II}}\text{NTA}$ yields $\Delta H^\ddagger = 14 \pm 2$ kcal/mol and $\Delta S^\ddagger = -4 \pm 8$ eu. The activation parameters are consistent with a mechanism involving binding of $\text{Cu}(\text{II})$ to the protein, because such binding would be expected to dislodge water molecules from both reactant surfaces.

NMR experiments were performed to identify the $\text{Cu}(\text{II})$ binding site. The effect of $\text{Cu}^{\text{II}}\text{NTA}$ on the aromatic region of the ^1H NMR spectrum of oxidized cytochrome b_5 is shown in Figure 4. The three well-resolved singlets (labeled 1–3)

Table II: Rate and Binding Constants for Oxidation of Cytochrome b_5 by $\text{Cu}^{\text{II}}\text{L}$ at 25 °C ($\mu = 0.1$ M)

L	pH	k_{et} (s^{-1})	K (M^{-1})
NTA	6.0	1.1	3.1×10^2
	7.0 ^a	0.05	8.6
His	7.0	0.2	2.6×10^3
ATP	7.0	0.6	4.5×10^3

^a Observed rate constants at different ionic strengths [$k_{\text{obsd}} \times 10^3$ (s^{-1}), μ (M)]: 0.6 ± 0.1 , 0.05; 1.5 ± 0.3 , 0.1; 1.3 ± 0.1 , 0.2; 1.6 ± 0.1 , 0.3. [$\text{Cu}^{\text{II}}\text{NTA}$] = 0.3 mM.

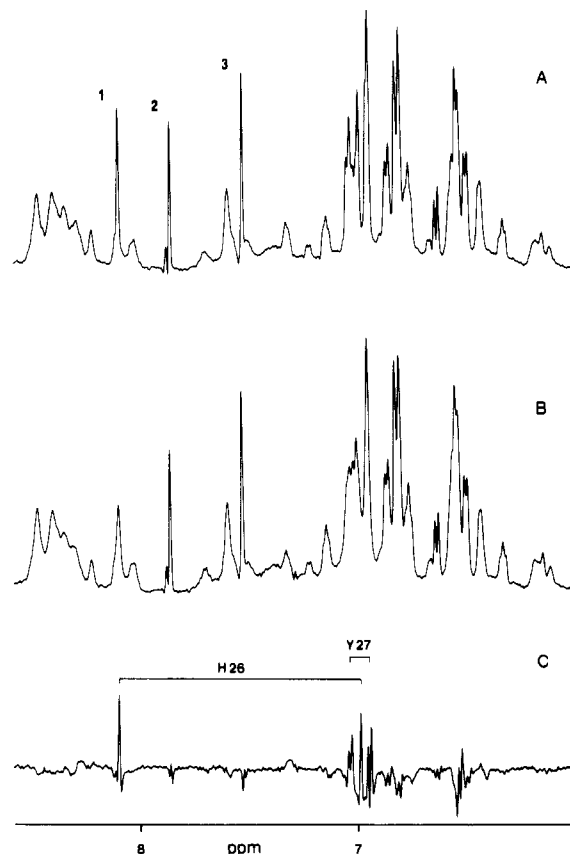


FIGURE 4: Aromatic region of the 500-MHz ^1H NMR spectrum of oxidized cytochrome b_5 : (A) Native cytochrome b_5 at 24 °C (pH 6.9). The C β H proton resonances of the three surface histidines are labeled 1–3. (B) Cytochrome b_5 with $\text{Cu}^{\text{II}}\text{NTA}$ (0.11 mM). (C) Difference spectrum, A – B. The resonances of His-26 and Tyr-27 that are broadened by $\text{Cu}^{\text{II}}\text{NTA}$ are indicated in the difference spectrum.

originate from the C β H protons of the three surface histidine residues (His-15, His-26, and His-80) that are distant from the paramagnetic heme group. Titration with $\text{Cu}^{\text{II}}\text{NTA}$ causes significant broadening of resonance 1, while resonances 2 and 3 remain unaffected even at high concentrations of the copper complex. By use of difference spectroscopy (Figure 4), broadening of an additional singlet and of two doublet resonances of a tyrosine residue is observed. It is apparent from the NMR titration experiment that only one surface histidine residue is affected on binding of $\text{Cu}^{\text{II}}\text{NTA}$ to cytochrome b_5 .

Two-dimensional NMR experiments were performed to identify the histidine and tyrosine residues at the $\text{Cu}^{\text{II}}\text{NTA}$ binding site. Assignments were based on nuclear Overhauser effects (NOE) between the proton resonances of the histidines and those arising from surrounding amino acid side chains. The NOE data were interpreted on the basis of interproton distances calculated from the crystal structure of cytochrome b_5 (Mathews et al., 1972). Amino acid spin systems were identified from double-quantum and relayed coherence transfer

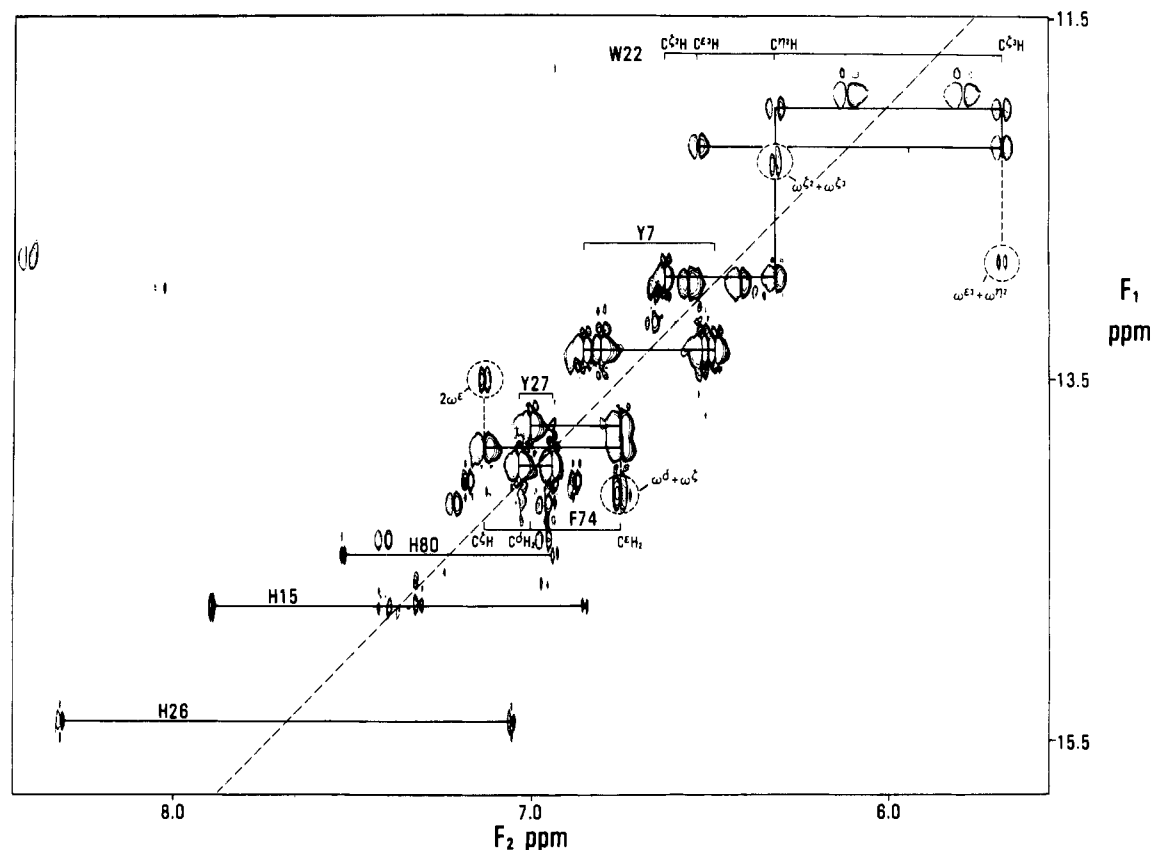


FIGURE 5: Region of the phase-sensitive double-quantum spectrum of oxidized cytochrome b_5 at 24 °C in potassium phosphate buffer (50 mM, pH 7.0) in $^2\text{H}_2\text{O}$. The multiple-quantum excitation period was $\tau = 40$ ms. A total of 512 t_1 values were recorded with 2048 complex points and 64 scans for each t_1 value. The spectral width in ω_2 was 6494 Hz and in ω_1 was 12988 Hz. The sloping, dashed line represents the double-quantum pseudodiagonal ($\omega_1 = 2\omega_2$); the direct (solid line) and remote (dashed line and circled) connectivities for Trp-22, Tyr-7, Tyr-27, Phe-74, and the three surface histidines (His-15, His-26, and His-80) are indicated. Both positive and negative contour levels are drawn.

spectra. Assignment of the resonances of the only tryptophan residue in cytochrome b_5 (Trp-22) was straightforward. Observation of all of the expected direct and remote connectivities in the double-quantum spectrum (Figure 5) makes the assignment unambiguous. The C^5H and C^6H doublets were distinguished on the basis of a strong NOE (not shown) from the resonance at 6.65 ppm to an Ile C^6H_3 triplet at -1.17 ppm. The X-ray structure shows the C^6 atom of Ile-76 close to the C^5 of Trp-22 and allows specific assignment of these resonances. Our assignments for Ile-76 agree with those made previously on the basis of ring current shifts (Keller & Wüthrich, 1980).

Connectivities between the C^5H and C^6H resonances of the imidazole rings of the three histidines are also observed in the double-quantum spectrum. The two singlets that are broadened by $\text{Cu}^{\text{II}}\text{NTA}$ originate from C^5H and C^6H resonances of the same histidine residue. The aromatic proton resonances of all four tyrosine residues were identified in the double-quantum spectrum.

Specific assignments for the histidine resonances are based on NOE connectivities. Strong NOE cross-peaks are observed between resonances of Trp-22 and the C^6H_2 and C^5H_2 resonances of tyrosine (at 6.51 and 6.87 ppm) and the histidine C^5H resonance labeled 2 in Figure 4 (Figure 6). On the basis of the X-ray structure, these residues are assigned unambiguously to Tyr-7 and His-15, respectively. These are the only aromatic residues in proximity to Trp-22.

The C^5H resonance labeled 1 in Figure 4 and the C^6H resonance of the same histidine show strong NOEs to a methyl group resonance at 0.40 ppm (Figure 7). Double-quantum and relayed coherence transfer spectra (not shown) show that

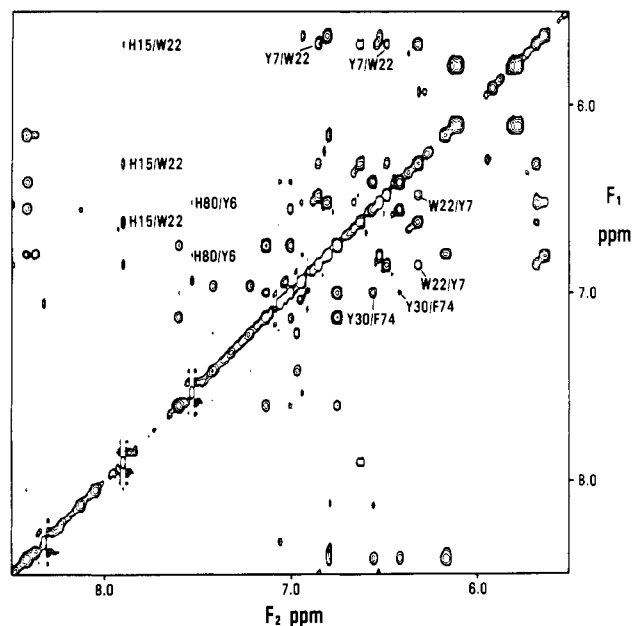


FIGURE 6: Region of a phase-sensitive NOESY spectrum of cytochrome b_5 at 24 °C in potassium phosphate buffer (50 mM, pH 7.0) in $^2\text{H}_2\text{O}$. The mixing time $\tau_m = 200$ ms. A total of 996 t_1 values were recorded with 2048 complex points and 64 scans for each t_1 value. The spectral width in ω_1 and ω_2 was 13889 Hz.

this methyl group resonance arises from a threonine spin system with C^5H and C^6H resonances at 2.88 and 3.79 ppm, respectively. The X-ray structure shows that His-26 and Thr-55 are close enough to give rise to the observed NOEs.

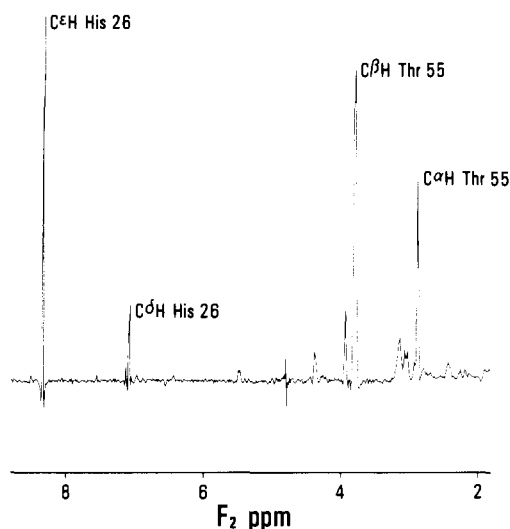


FIGURE 7: Row of the phase-sensitive NOESY spectrum taken at the ω_1 frequency of the $C^{\gamma}H_3$ resonance of Thr-55 ($\omega_1 = 0.40$ ppm). The experimental conditions are given in the legend of Figure 6.

The remaining histidine resonances at 7.52 and 6.95 ppm are assigned to His-80, which the X-ray structure shows is too distant from either Thr or Trp residues to give rise to the above NOEs. Weak NOE cross-peaks are observed between the $C^{\alpha}H$ and $C^{\delta}H$ resonances of His-80 and the $C^{\alpha}H_2$ and $C^{\beta}H_2$ resonances of a tyrosine, which on the basis of the X-ray structure is assigned to Tyr-6.

The double-quantum spectrum shows that the two $Cu^{II}NTA$ -broadened doublets (7.04 and 6.95 ppm) originate from a tightly coupled tyrosine spin system, arising from either Tyr-27 or Tyr-30. The resonances of Tyr-30 are readily identified (6.42 and 6.57 ppm) on the basis of strong NOE connectivities both to $C^{\delta}H_3$ resonances of Leu-25 assigned by Keller and Wüthrich (1980) and to the $C^{\beta}H_2$ resonance of Phe-74. From the X-ray structure only Tyr-30 and Phe-74 are sufficiently close to give rise to observable NOEs. The aromatic spin system of Phe-74, the only phenylalanine residue distant from the paramagnetic heme (~ 10 Å from the heme center), is readily assigned from the double-quantum spectrum. Thus by elimination, the tyrosine resonances broadened by $Cu^{II}NTA$ originate from Tyr-27. A direct assignment based on NOEs from Tyr-27 resonances cannot be made at present. However, from the X-ray structure it is expected that binding of $Cu^{II}NTA$ to His-26 will broaden the resonances of the adjacent Tyr-27. These residues are at positions $i + 1$ and $i + 2$ of a reverse turn, and the side chains form a suitable binding site for the $Cu(II)$ complex. The chemical shifts of the assigned resonances of oxidized cytochrome b_5 are given in Table III.

The NMR experiments show unequivocally that the $Cu^{II}NTA$ binding site is in the region of His-26 and Tyr-27. This site is located on the surface of the protein at a distance of approximately 13 Å from the heme iron atom (Figure 8). Since the rate of a long-range electron transfer depends strongly on the reduction potential of the metal complex that is bound to the protein (Lieber et al., 1987), the observed facile oxidation of the b_5 heme indicates that the reduction potential of the docked $Cu(II)$ is shifted to a more positive value. Protein chelation of $Cu(II)$ in the His-26 (Tyr-27) region apparently provides an environment that is favorable for $Cu(I)$, and this environment may even lower the reorganization energy for electron transfer to $Cu(II)$. The combination of increased driving force and lowered reorganization energy would strongly favor long-range $Fe(II)$ to $Cu(II)$ electron transfer.

Table III: Proton Resonance Assignments for Oxidized Cytochrome b_5 at 24 °C (p^2H 6.93)

residue	chemical shifts (ppm)
His-15	$C^{\alpha}H$, 7.89; $C^{\delta}H$, 6.86
His-26	$C^{\alpha}H$, 8.32; $C^{\delta}H$, 7.08
His-80	$C^{\alpha}H$, 7.52; $C^{\delta}H$, 6.95
Tyr-6	$C^{\beta}H_2$, $C^{\alpha}H_2$, 6.53, 6.81
Tyr-7	$C^{\beta}H_2$, $C^{\alpha}H_2$, 6.51, 6.87
Tyr-27	$C^{\beta}H_2$, $C^{\alpha}H_2$, 7.04, 6.95
Tyr-30	$C^{\beta}H_2$, $C^{\alpha}H_2$, 6.42, 6.57
Trp-22	$C^{\delta}H$, 6.65; $C^{\alpha}H$, 6.33; $C^{\beta}H$, 5.69; $C^{\gamma}H$, 6.55
Phe-74	$C^{\alpha}H_2$, 7.01; $C^{\beta}H_2$, 6.76; $C^{\delta}H$, 7.14
Leu-25	$C^{\gamma}H$, -0.17; $C^{\delta}H_3$, -2.14, -0.84
Thr-55	$C^{\alpha}H$, 2.88; $C^{\beta}H$, 3.79; $C^{\gamma}H_3$, 0.40
Ile-76	$C^{\delta}H_3$, -1.17; $C^{\gamma}H$, 0.16, -0.10

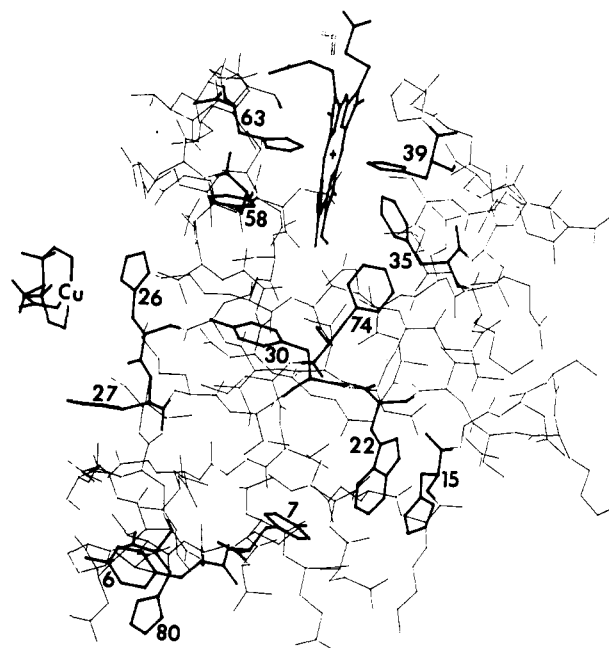


FIGURE 8: Structure of cytochrome b_5 . Aromatic and histidine residues and the heme group are highlighted. The protein forms a spherate ellipsoid with a diameter of 31 Å and a height of 38 Å. A $Cu^{II}NTA$ complex is docked at His-26.

ACKNOWLEDGMENTS

We thank Kaspar Hegetschweiler for helpful discussions throughout the course of this work. L.S.R. acknowledges the I. W. Killiam Foundation and the Medical Research Council of Canada for postdoctoral fellowships.

Registry No. $Fe^{III}NTA$, 16448-54-7; $Fe^{III}ATP$, 3269-25-8; $Cu^{II}NTA$, 34831-02-2; $Cu^{II}ATP$, 18925-86-5; $Cu^{II}His$, 13870-80-9; Cu , 7440-50-8; cytochrome b_5 , 9035-39-6.

REFERENCES

- Bonfils, C., Balny, C., & Maurel, P. (1981) *J. Biol. Chem.* 256, 9457–9465.
- Braunschweiler, L., Bodenhausen, G., & Ernst, R. R. (1983) *Mol. Phys.* 48, 535–560.
- Egyed, A., & Saltman, P. (1984) *Biol. Trace Elem. Res.* 6, 357–364.
- Eich, G., Bodenhausen, G., & Ernst, R. R. (1982) *J. Am. Chem. Soc.* 104, 3731–3732.
- Hegetschweiler, K., Saltman, P., Dalvit, C., & Wright, P. E. (1987) *Biochim. Biophys. Acta* 912, 384–397.
- Keller, R. M., & Wüthrich, K. (1980) *Biochim. Biophys. Acta* 621, 204–217.
- Kumar, A., Ernst, R. R., & Wüthrich, K. (1980) *Biochem. Biophys. Res. Commun.* 95, 1–6.

- Lieber, C. M., Karas, J. L., & Gray, H. B. (1987) *J. Am. Chem. Soc.* 109, 3778-3779.
- Mathews, F. S., Argos, P., & Levine, M. (1972) *Cold Spring Harbor Symp. Quant. Biol.* 36, 387-395.
- Mayo, S. L., Ellis, W. R., Jr., Crutchley, R. J., & Gray, H. B. (1986) *Science (Washington, D.C.)* 233, 948-952.
- Reid, L. S., & Mauk, A. G. (1982) *J. Am. Chem. Soc.* 104, 841-845.
- Reid, L. S., Taniguchi, V. T., Gray, H. B., & Mauk, A. G. (1982) *J. Am. Chem. Soc.* 104, 7516-7519.
- Rifkind, J. M. (1981) *Met. Ions Biol. Syst.* 12, 191-232.
- Wagner, G. (1983) *J. Magn. Reson.* 55, 151-156.

Labeling of the ATP Synthase of *Escherichia coli* from the Head-Group Region of the Lipid Bilayer[†]

Robert Aggeler, Yu-Zhong Zhang, and Roderick A. Capaldi*

Institute of Molecular Biology, University of Oregon, Eugene, Oregon 97403

Received March 24, 1987; Revised Manuscript Received May 18, 1987

ABSTRACT: The isolated and membrane-bound forms of the adenosinetriphosphatase of *Escherichia coli* (ECF₁ and ECF₁F₀, respectively) have been reacted with two lysine-specific reagents, sodium hexadecyl 4-[³H]formylphenyl phosphate (HFPP) and sodium methyl 4-[³H]formylphenyl phosphate (MFPP), and with the photoreactive reagent 1,2-[³H]dipalmitoyl-*sn*-glycerol 3-[[[(4-azido-2-nitrophenyl)amino]ethyl]phosphate] (arylazidoPE). HFPP and arylazidoPE are amphipathic molecules, inserting by their hexadecyl moieties (one and two chains, respectively) into the lipid bilayer, with the reactive groups intercalated among the phospholipid head groups. MFPP is the water-soluble analogue of HFPP. The labeling patterns of ECF₁F₀ obtained with HFPP and arylazidoPE were very similar; in both cases the α and β subunits of the F₀ part were the most heavily labeled polypeptides of the complex. Models of subunit α , arranged in six transmembrane helices, place most of the lysines in the head-group region, available for reaction with HFPP. Subunits α and β of the ECF₁ part were very poorly labeled in comparison to the α and β subunits, together incorporating only 4% as much HFPP and 7.5% as much arylazidoPE as the two F₀ subunits together on a protein mass basis. Trypsin cleavage studies localized any labeling of the α subunit by arylazidoPE to the N-terminal 15 residues of this polypeptide. When MFPP was used, the α and β subunits were very much more reacted than the F₀ subunits. This implies that most of the mass of the α and β subunits in ECF₁F₀ is above the membrane and not in contact with the bilayer surface. One subunit of ECF₁, the δ subunit, was heavily labeled by HFPP and MFPP in free ECF₁ but was shielded from reaction with both of these probes and with arylazidoPE in ECF₁F₀ preparations. The implication is that the δ subunit, a link between ECF₁ and F₀, is shielded by protein-protein interactions, at least in the lipid head-group region of the bilayer.

The adenosine 5'-triphosphate (ATP) synthase of *Escherichia coli* (EF₁F₀) is organized into two major domains, the F₁ part, extrinsic to the membrane lipid bilayer and containing the catalytic sites, and an F₀ part, intrinsic to the membrane bilayer continuum and involved in proton translocation. ECF₁ contains five different subunits, α , β , γ , δ , and ϵ , in the molar ratio 3:3:1:1:1. F₀ contains three different polypeptides, a , b , and c , in the molar ratio 1:2:10 or 12 [reviewed in Senior and Wise (1983), Walker et al. (1984), and Bragg (1984)]. The F₁ part of the ATP synthase is very similar in all organisms, with the same number of subunits and with considerable sequence conservation of the α and β polypeptides (Walker et al., 1984). F₁, with a molecular weight of 380 000, is a large globular structure. X-ray studies of the rat liver enzyme indicate that the protein is an ellipsoid with dimensions of around 110 × 80 Å (Amzel et al., 1982). How the F₁ is oriented in the F₁F₀ complex is not known.

Electron microscopy studies of the ATP synthases from bacteria, mitochondria, and chloroplasts show F₁ associated

with the membrane part (F₀) through an extension or stalk (Soper et al., 1979; Kagawa et al., 1976; Gogol et al., 1987). Reconstitution studies indicate that both the δ and ϵ subunits are important for the interaction of ECF₁ with F₀ (Sternweis, 1978). Also, protease digestion of subunit b in ECF₁-depleted membranes has been shown to prevent rebinding of ECF₁ to F₀ (Perlin et al., 1983; Hermolin et al., 1983). Thus the δ , ϵ , and b subunits may all contribute to the stalk that links F₁ and F₀.

The arrangement of subunits in ECF₁F₀ has been probed previously by chemical labeling (Hoppe & Sebald, 1984; Bragg, 1984), cross-linking (Aris & Simoni, 1983; Hermolin et al., 1983; Bragg & Hou, 1980), antibody binding, and protease digestion experiments (Dunn et al., 1980; Smith & Sternweis, 1982). In this study we have used amphipathic reagents to label those parts of the protein at the lipid head group-water interface of the membrane. One reagent is 1,2-[³H]dipalmitoyl-*sn*-glycerol 3-[[[(4-azido-2-nitrophenyl)amino]ethyl]phosphate] (arylazidoPE); the other is the novel protein modifying reagent sodium hexadecyl 4-[³H]-formylphenyl phosphate, introduced recently by Keana, Griffith, and associates (McMillen et al., 1986). Our results are interpreted in terms of the proximity of the F₁ to the F₀

[†] This research was supported by National Institutes of Health Grant HL-22050. R.A. was supported by a fellowship from the Swiss National Science Foundation.